J Mater Sci (2017) 52:5788–5798

Comprehensive approaches to three-dimensional flexible supercapacitor electrodes based on MnO_2/carbon nanotube/activated carbon fiber felt

Jingwen Zhang[1], Liubing Dong[1,2], Chengjun Xu[1,*], Jianwu Hao[1], Feiyu Kang[1,2], and Jia Li[1]

[1] *Graduate School at Shenzhen, Tsinghua University, Shenzhen 518055, China*
[2] *School of Materials Science and Engineering, Tsinghua University, Beijing 100084, China*

Received: 6 December 2016
Accepted: 16 January 2017
Published online: 23 January 2017

ABSTRACT

With the fast development of portable and wearable devices, flexible supercapacitor electrodes are widely researched. Here, comprehensive approaches were designed to introduce carbon nanotube (CNT) and/or MnO_2 into activated carbon fiber felt (ACFF) using "dipping and drying" method. Differences on micro-morphologies and electrochemical characteristics for prepared textiles were compared. High-performance flexible MnO_2/CNT/ACFF composite electrodes were synthesized by introducing CNT and MnO_2/CNT fillers successively. Compared with original ACFF textiles, significant improvements in electrochemical performance were achieved. Areal capacitance, energy density and power density of the composite textiles reached as high as 4148 mF cm^{-2}, 141 μWh cm^{-2} and 4466 μW cm^{-2}, respectively. Furthermore, flexible supercapacitors were fabricated based on the composite textile electrodes and gel electrolytes. When being bent at different angles or suffering deformations such as bending for 100 cycles, the flexible supercapacitors preserve almost all the capacitance, which indicates the excellent flexibility of the composite textile electrode. This work provides various approaches to design composite textiles, and the prepared MnO_2/CNT/ACFF composite textile may be a promising electrode material for high-performance flexible supercapacitors.

Introduction

Flexible electrodes used for supercapacitors have received great interest with the development of portable and wearable electronic devices in recent years [1–3]. However, for most flexible electrodes, especially for fiber-like [4–6] and paper-like [7–9] ones, the energy output for single electrode is limited and not suitable to use for large-scale devices [3, 10]. Therefore, three-dimensional (3D) flexible electrodes arouse an increasing attention [3, 11–14]. In general, 3D electrodes are composed of body materials and active fillers [15–17]. Body materials include cotton,

Address correspondence to E-mail: vivaxuchengjun@163.com

DOI 10.1007/s10853-017-0813-3

carbon cloth (CC), sponge-like monoliths [18–20], etc. Fillers involve activated carbon (AC), metallic oxides, etc. [3, 21–24]. For most 3D electrode, the weight of electrochemical passive body material may be an obstacle to the specific capacitance of the whole electrode [3, 25].

Flexible supercapacitor electrodes based on activated carbon fiber felt (ACFF) were reported lately by our laboratory [26]. ACFF provides an areal capacitance of ~2000 mF cm^{-2}. The porosity of ACFF is ~95%, which ensures the ion movements within the material and allows the introduction for additives into the textile [27, 28]. In the previous study, carbon nanotube (CNT) and graphene (GN) were introduced into ACFF using freeze-drying method and resulted in significant enhancements in electrochemical performances [26]. However, the CNT and GN only improve the electrical conductivity and possess nearly no capacitance, and the high porosity of ACFF may indicate a possibility for introducing more fillers into the matrix.

To further improve the electrochemical performances of composite textiles and make use of the porous matrix, MnO_2 was considered to be introduced into ACFF, as MnO_2 preserves high theoretical capacitance [29–31]. Different procedures were researched to fabricate a most promising composite textile using CNT and MnO_2. It was found out that among all the prepared textiles, MnO_2/CNT/ACFF composite textiles fabricated by dipping ACFF into CNT and MnO_2/CNT suspensions process the best electrochemical properties. The comparison of different approaches may provide a train of thought to design a composite material, and the fabricated composite textile which achieved significant improvements in electrochemical performances may be a promising material for flexible supercapacitors.

Experimental

Preparation of MnO_2/CNT suspensions

ACFF textiles used in the experiments were obtained from Shenzhou Carbon Fiber Co., Ltd, China. 5 wt% CNT paste (Model: NTP2021) was purchased from Shenzhen Nanotech Port Co., Ltd. In order to get MnO_2/CNT suspensions, 12 g 5 wt% CNT pastes and 50 ml 0.4 mol L^{-1} $KMnO_4$ aqueous solution were mixed at ambient temperature and stirred for 12 h to speed up reactions and disperse extra CNTs and MnO_2 uniformly [32–35]. Filtration method was used to get reaction products, and during this period, products were washed by deionized water for several times to ensure no MnO_4^- exists. Products were then dried at 80 °C and dispersed in deionized water to get suspensions with the concentration of 2 wt%. 1 wt% CNT suspensions were prepared by mixing 5 wt% pastes with deionized water.

Preparation of different textiles

CNTs and MnO_2 were introduced into ACFF textiles by a "dipping and drying" method. The preparation procedures for different textiles are displayed in Fig. 1a. ACFF were dipped into prepared CNT suspension for 1 min and dried at 80 °C. The prepared CNT/ACFF textiles are denoted as "FC" (procedure 1). "FKM" was prepared by directly dipping ACFF into 0.1 M $KMnO_4$ aqueous solution for 1 min, washed by deionized water thoroughly and dried at 80 °C (procedure 2). Textiles denoted as "FM" were prepared by dipping ACFF textiles into prepared MnO_2/CNT suspensions (procedure 3). "FCM" textiles were fabricated by a two-step procedure, dipping ACFF into the two kinds of suspensions separately (procedure 4).

Characterizations of prepared textiles

Morphologies of CNT, MnO_2/CNT fillers, ACFF and prepared composite textiles were observed using scanning electron microscopy (SEM). Energy-dispersive spectroscopy (EDS) mapping was conducted on FKM, FM and FCM textiles to show the distribution of C, O, Mn and K elements. X-ray diffraction (XRD) was performed on MnO_2/CNT powders and FKM textiles to determine the crystal structure of generated MnO_2. An electronic balance was used to conduct the weights of textiles both before and after preparing processes. And areal densities (D) for different textiles were calculated baed on the results. Thermal gravimetric analyses (TG) were conducted on FM and FCM textiles. Electrical conductivities of all textiles were measured in a four-point probe instrument. The specific surface area and pore-size distribution of different textiles were described in a Brunauer–Emmett–Teller (BET) analyzer by N_2 adsorption tests.

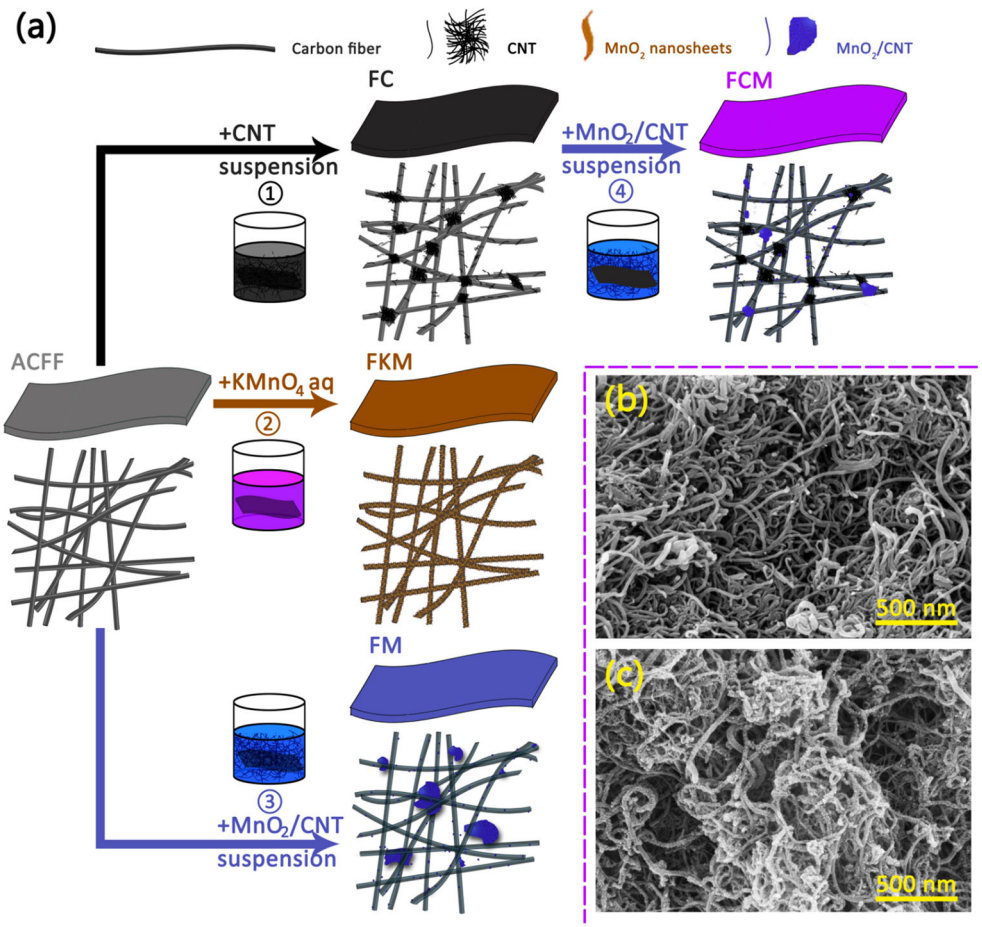

Figure 1 Schematics of different textiles, including fabrication processes and microstructures (**a**). SEM images of CNT fillers (**b**) and MnO_2/CNT fillers (**c**).

Coin-cell supercapacitors were prepared to test electrochemical performances of the materials. CNT powders (dried from CNT paste) or MnO_2/CNT powders were mixed with acetylene black and polyvinylidene fluoride (PVDF) by a weight ratio of 8:1:1, respectively. *N*-Methylpyrrolidone (NMP) was used to disperse the powder thoroughly. The mixtures were coated on stainless steel foil and dried at 110 °C for at least 10 h to form CNT or MnO_2/CNT electrodes. Symmetric coin-cell supercapacitors with 1 M H_2SO_4 electrolyte were prepared to characterize the electrochemical performances of CNT electrodes, MnO_2/CNT electrodes and various textile electrodes, and the area of each electrode is the same ~1.131 cm^2 and each electrode weights 20–30 mg for different textiles. Cyclic voltammetry (CV) tests and galvanostatic charge–discharge measurements were performed at a VMP3 electrochemical station. Areal capacitances (C_S), energy densities (E_S) and power densities (P_S) of different electrodes/supercapacitors were then calculated.

Results and discussion

Morphology of textiles

Microstructures of CNT and MnO_2/CNT fillers are shown in Fig. 1b, c. MnO_2 grains on the surface of CNTs are observed in MnO_2/CNT fillers. X-ray diffraction patterns of MnO_2/CNT fillers and FKM textile are shown in Fig. S2. From the XRD pattern, a type of birnessite MnO_2 is found in both materials. SEM images of different textiles and surface morphologies of carbon fibers are presented in Fig. 2a–e and their insets. ACFF is constructed by many disordered carbon fibers and has high porosity. The surface of carbon fibers is smooth. For composite textiles, several fillers can be found on the surface of carbon fibers. Flaky joints between carbon fibers distributed by CNTs are found in FC, and these joints may help increase the electronic conductivity. In FKM, the main structure of ACFF keeps its status and almost MnO_2 grew uniformly in the form of

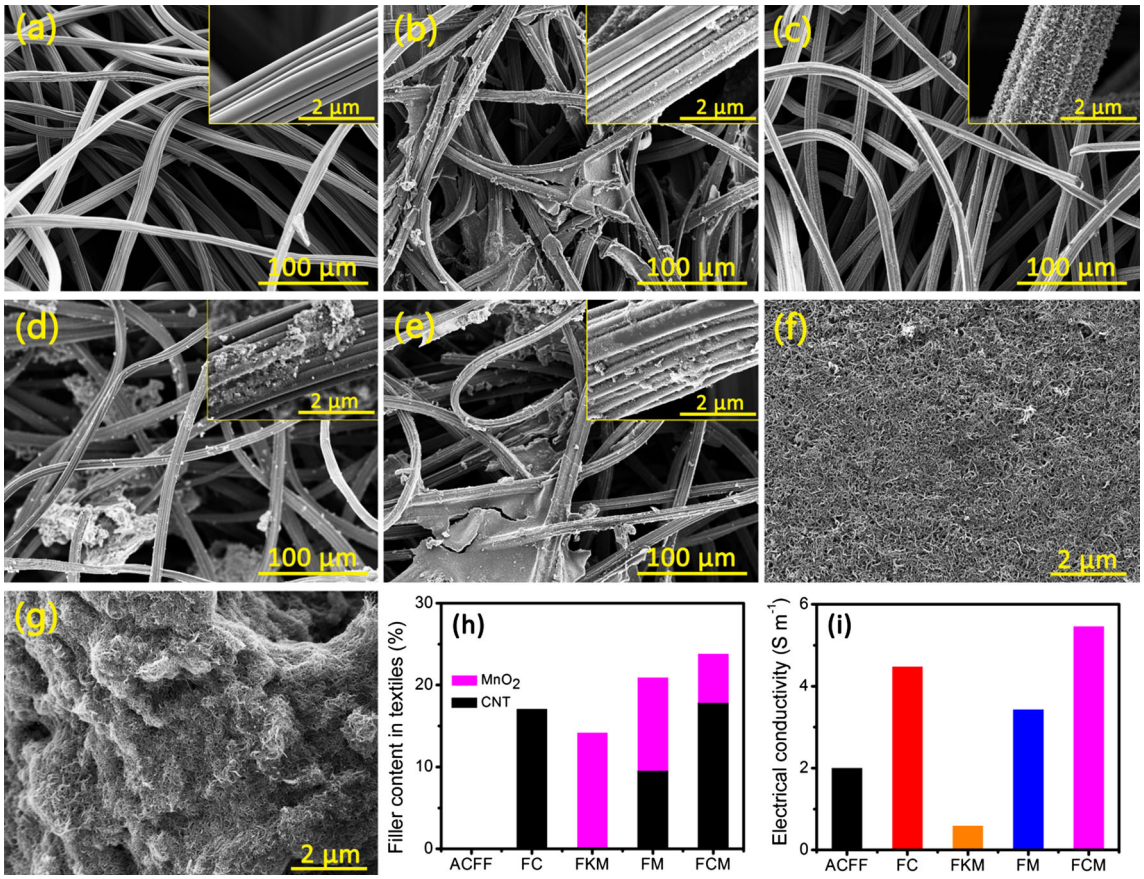

Figure 2 SEM images of ACFF (**a**), FC (**b**), FKM (**c**), FM (**d**), and FCM textiles (**e**), *insets* are magnified images of single fiber for each textile; **f** and **g** are detailed images of two main morphologies in Fig. 2e (FCM textile); weight fraction composition (**h**) and electrical conductivity of textiles (**i**).

nanosheets on the surface of carbon fibers. However, this may cause a decrement in the electronic conductivity because of the low electronic conductivity of MnO_2. For FM, MnO_2/CNT fillers form irregular-shaped aggregations. In FCM textiles, both flaky joints between carbon fibers and irregular-shaped aggregations are observed. The detailed images of the two kinds of morphologies are presented in Fig. 2f, g. The distribution of MnO_2 in FCM and comparison of the morphologies among FC, FCM and FKM are further discussed in supporting information using EDS results (Fig. S3) and detailed SEM images (Fig. S4).

The percentage of fillers in composite textiles (Fig. 2h) ranges from ~15 to ~25%. Detailed compositions of different textiles were calculated by computing methods given in supporting information using TG results shown in Fig. S2. Electronic conductivity values of different textiles are given in Fig. 2i. Compared with ACFF, electronic conductivities of FKM suffered a significant decrement. For other composite textiles, the introduction of fillers into textiles results in an improvement in electronic conductivity because of the introduction of CNT fillers [36]. Table 1 presents the values of areal density (D), S_{BET}, V_p and d of different textiles. For all the composite textiles, areal density shows an increment compared with ACFF because of the introduction of fillers. ACFF preserves a high S_{BET} of ~1700 $m^2\ g^{-1}$, while S_{BET}, V_p and d values shows rather smaller values than ACFF. It can be seen from

Table 1 D, S_{BET}, V_p and d values of different textiles

Sample	ACFF	FC	FKM	FM	FCM
D (g m^{-2})	173	209	199	219	227
S_{BET} ($m^2\ g^{-1}$)	1692	1091	779	795	749
V_p ($cm^3\ g^{-1}$)	1.90	0.77	0.59	0.46	0.52
d (nm)	4.50	2.83	3.01	2.29	2.79

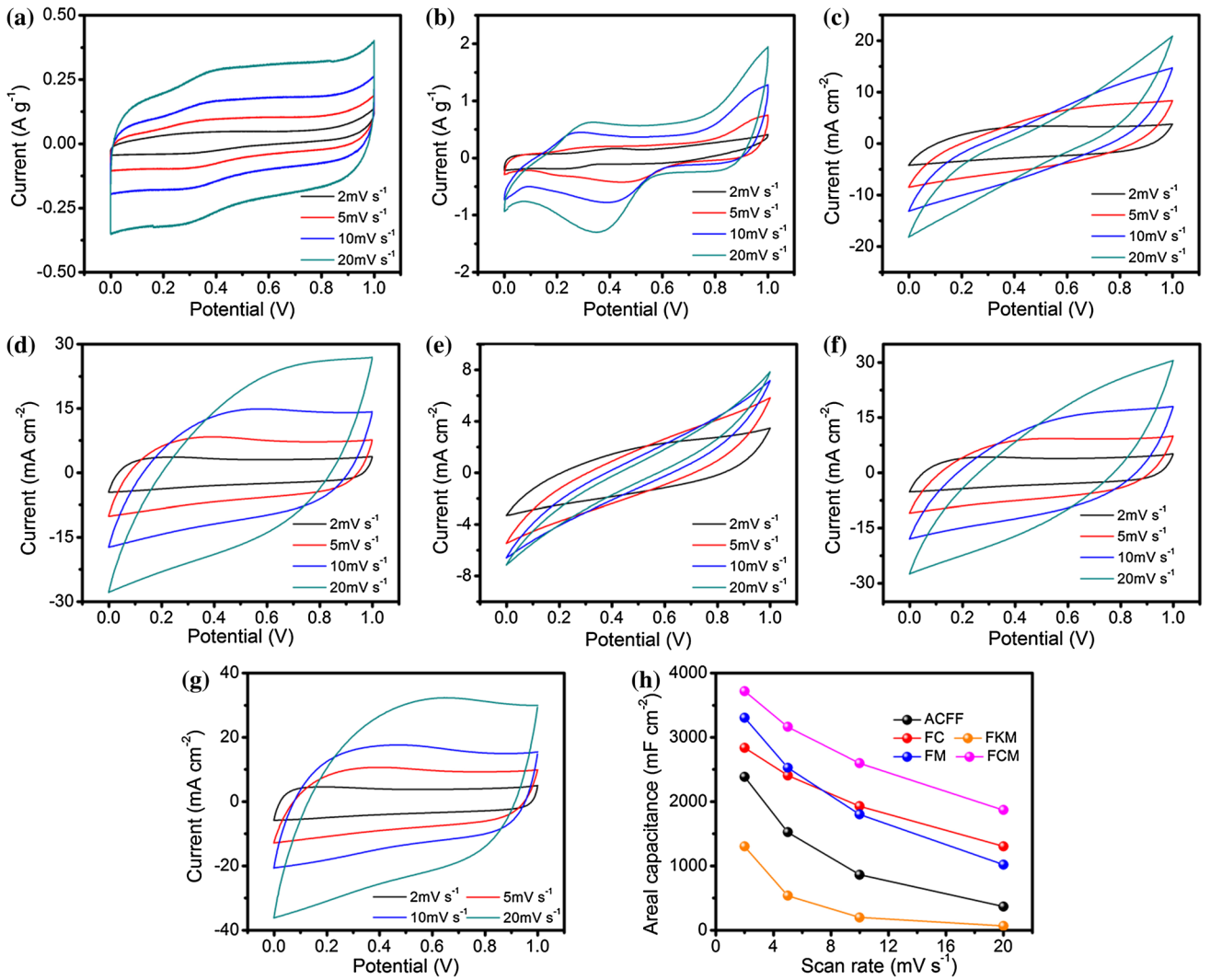

Figure 3 CV curves at different scan rates of CNT (**a**), MnO_2/CNT (**b**), ACFF (**c**), FC (**d**), FKM (**e**), FM (**f**), and FCM (**g**). Areal capacitances of each electrode calculated from CV curves (**h**).

SEM images that some filler covers on the surface of carbon fibers, which may cause the decrement in S_{BET} value. The aggregations occupy some holes in ACFF, which leads V_p and d values to decrease in composite textiles.

Electrochemical performance of textile electrodes

CV curves of CNT and MnO_2/CNT fillers are displayed in Fig. 3a, b. The CV curves of CNT show nearly rectangular shape at different scan rates, indicating a double-layer capacitive behavior. Its capacitance is $\sim$20 F g^{-1}, similar to commercial CNTs reported [37–39]. Capacitance of MnO_2/CNT, calculated from CV curve at 2 mV s^{-1}, is $\sim$150 F g^{-1}, much higher than CNT.

CV scans were performed on different textiles at scan rates from 2 to 20 mV s^{-1}, and results are shown in Fig. 3c–g. Capacitance of ACFF is $\sim$2300 mF cm^{-2} at 2 mV s^{-1}, and obvious deviations of CV curves are observed at higher scan rates, indicating poor rate performance of ACFF. As shown in Fig. 2d, CNT fillers can optimize the electrochemical performance of ACFF, including areal capacitance and rate performance, by enhancing the electronic conductivity of ACFF [26]. The capacitances of FKM are much lower compared with ACFF. It shows that introducing MnO_2 into ACFF by this method cannot improve the electrochemical performance (Fig. 2e). When MnO_2 is

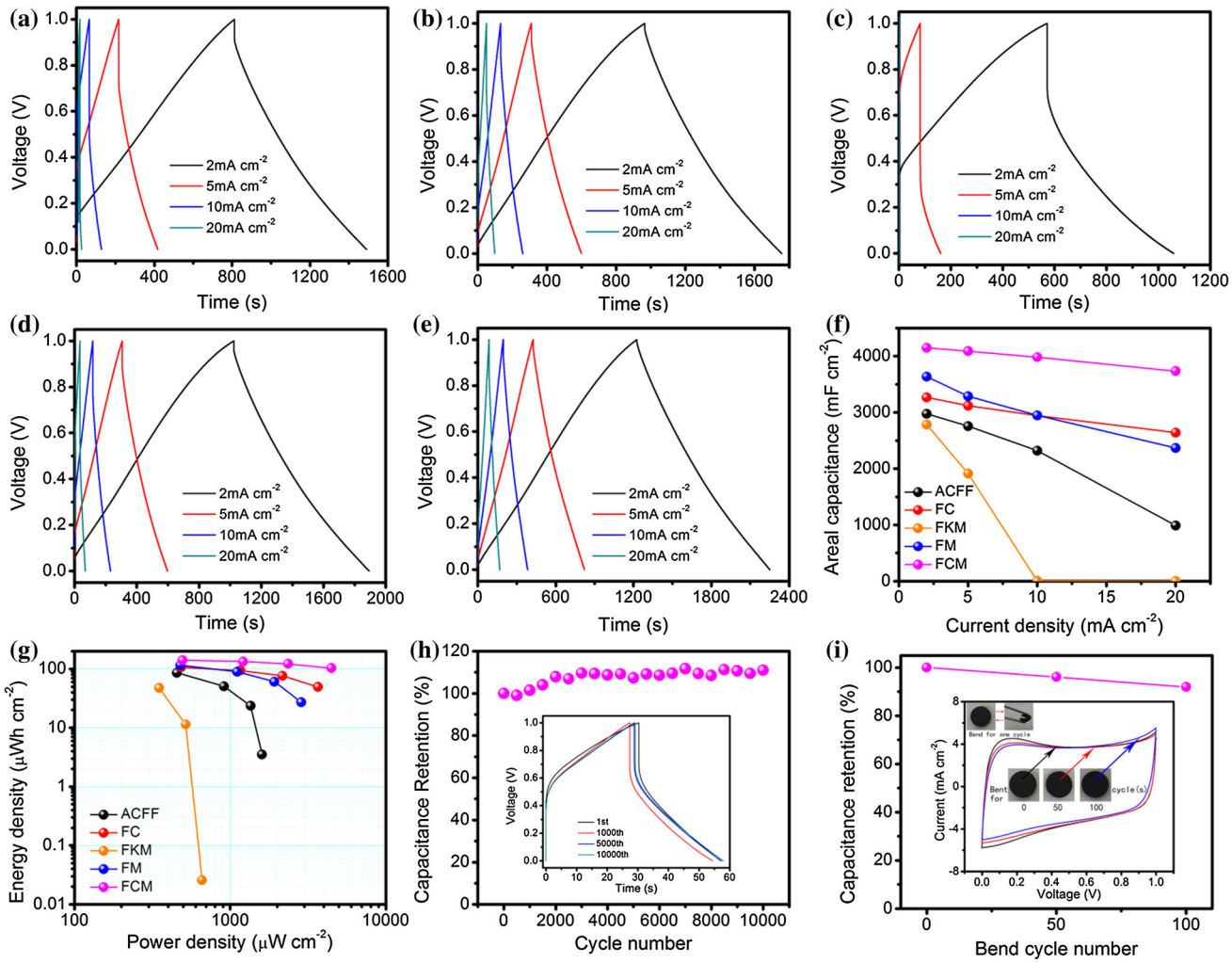

Figure 4 Voltage versus time curves from galvanostatic charge–discharge tests of different textiles, ACFF (**a**), FC (**b**), FKM (**c**), FM (**d**), and FCM (**e**). Areal capacitance of each supercapacitor calculated form galvanostatic charge–discharge tests (**f**); Ragone plots of the supercapacitors (**g**); cycle performances of FCM supercapacitor at a current density of 30 mA cm^{-2} for 10000 cycles (**h**); capacitance retention and CV curves at 2 mV s^{-1} of FCM electrodes after bending for 0, 50 and 100 cycles (**i**).

introduced in the form of MnO_2/CNT fillers, improvements in areal capacitance are displayed. However, at higher scan rates, the capacitance of FM decreases faster than FC. Among all the textiles, FCM shows most inspiring electrochemical performance. An areal capacitance result of ~3717 mF cm^{-2} at 2 mV s^{-1} is achieved. CV curves of FCM still remain nearly rectangular at a scan rate of 20 mV s^{-1}, demonstrating that the fillers provide crucial improvements on both areal capacitance and rate performance.

The results may be explained from Fig. 2 given before. To obtain high areal capacitance, introducing MnO_2 into the textile may be sufficient. However, FKM, which possesses the highest percentage of MnO_2, presents lowest areal capacitance among the textiles, even lower than ACFF. This is because the direct growth of MnO_2 on the surface of carbon fibers results in poor electronic conductivity of the composite textile. For FM and FCM, MnO_2 was introduced into ACFF in the form of MnO_2/CNT fillers. This results in less MnO_2 concentration in composite textiles but an improvement on electronic conductivity. For FC, FM and FCM, CNTs are all introduced into the textiles, but in two different forms: CNT or MnO_2/CNT fillers. Because of the existence of MnO_2, MnO_2/CNT fillers achieves higher capacitance but worse rate performance than CNT fillers, and this causes similar results for FC and FM textiles. And over-all improvements in the composite textiles are

Table 2 Comparison of prepared FCM supercapacitor with those in published papers

Electrode material	Electrolyte	D (g m^{-2})	C_S (F cm^{-2})	Maximum E_S (μWh cm^{-2})	Maximum P_S (mW cm^{-2})	Cyclic retention (%)	References
$NiCo_2O_4$/CC//porous GN paper	LiOH–PVA	55	0.39	333	62.1	96.8% 5000 cycles	[13]
$NiCo_2O_4$@$NiCo_2O_4$/ACT//ACT	KOH–PVA	27	0.48	224	22.5	98.0% 1000 cycles	[16]
Ni_3S_2@$Ni(OH)_2$/3D GN	KOH solution	37	4.70	260	18.4	99.1% 2000 cycles	[17]
Carbon particle/MnO_2/CC	Na_2SO_4 solution	131	0.11	63	18.3	97.3% 10000 cycles	[22]
SWNT/cotton	$LiPF_6$ solution	34	0.48	69	34.3	98% 130000 cycles	[23]
MnO_2/GN	Na_2SO_4 solution	110	1.42	–[a]	–	82% 5000 cycles	[24]
MnO_2/CNT/ACFC	KOH solution	–	2.54	57	16.3	96% 1500 cycles	[25]
CNT/ACFF	KOH solution	347	3.35	112	4.2	103% 1000 cycles	[26]
PPY/MnO_2/CC//AC/CC	H_3PO_4–PVA	–	1.41	630	0.9	98.6% 1000 cycles	[31]
MnO_2/CNT/paper	KOH solution	75	0.12	4	4.0	97.8% 20000 cycles	[41]
MnO_2/CNT/ACFF	H_2SO_4 solution	227	4.15	141	4.5	111.0% 10000 cycles	This work

Density results for all references; C_S for Ref. [16]; E_S, P_S results for Ref. [13, 16, 17, 22, 23] are not given directly in the references but can be counted out. Other figures presented in the table can be obtained directly from references

[a] This symbol means "not given or not clear and cannot be calculated from given data"

realized by introducing the two kinds of fillers together.

Galvanostatic charge–discharge measurements of different textile supercapacitors were taken to obtain the relationship curves of voltage *vs*. time, presented in Fig. 4a–e. Compared with ACFF, charge–discharge curves of FC, FM and FCM are more ideally V-shaped. Longer discharge times and smaller IR drops are attained. At 5 mA cm^{-2}, IR drop of ACFF and FKM is ~0.3 and ~0.7 V, respectively, while for supercapacitors fabricated with FC, FM and FCM composite textile electrodes, the IR drops are all ~0.1 V. The tendencies of the areal capacitances calculated by charge–discharge curves shown in Fig. 4f are similar with Fig. 3h and may be explained by the results of equivalent series resistance (ESR), which stands for the internal resistance of supercapacitors [40]. ESR is affected by many factors, including resistance of the electrode, ion diffusion resistances and interfacial resistances between electrodes and electrolyte. At 5 mA cm^{-2}, ESR values of ACFF, FC, FM, FKM and FCM supercapacitors are about 27, 7, 11, 59 and 4 Ω cm^{-2}, respectively. As a result, except for FKM, all composite textiles show better performances than ACFF. For FM, the ESR value is higher than FC and FCM, which is associated with the lower electronic conductivity of FM textile (Fig. 2i). As a result, the IR drops are larger and the rate performances are not so desirable at larger current densities. FC and FCM are similar with each other on rate performances, and the differences of capacitances are mainly caused by the contribution of MnO_2 in MnO_2/CNT fillers. A capacitance of 4148 mF cm^{-2} is achieved for FCM at the scan rate of 2 mA cm^{-2}.

Because of the large specific capacitances, high energy densities and power densities are obtained. Ragone plots of prepared supercapacitors are shown in Fig. 4g. Compared with ACFF, FC and FCM show considerably well performances. For instance, the

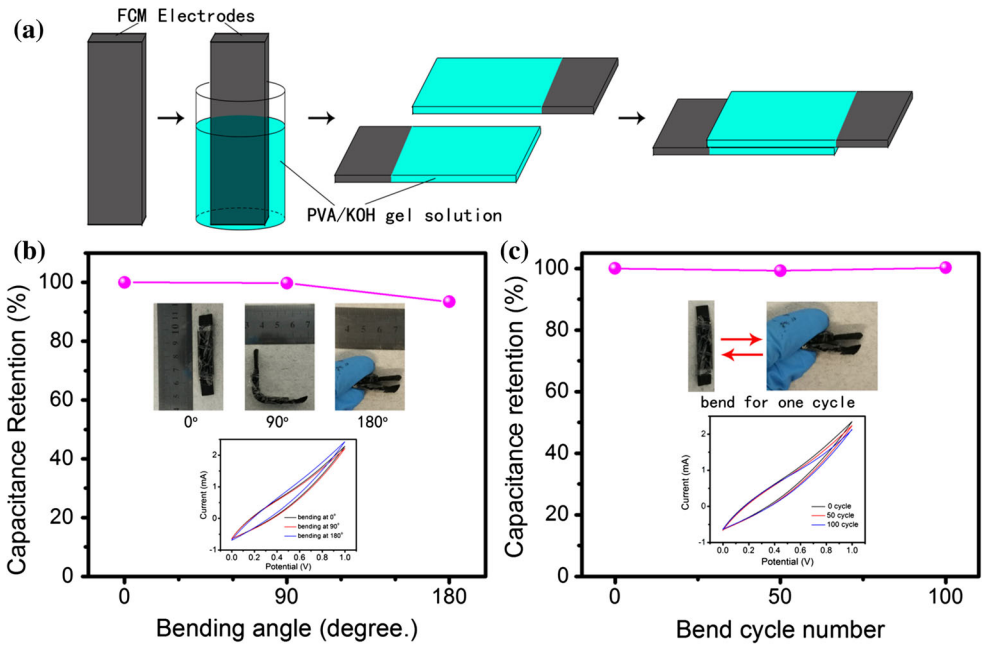

Figure 5 Fabrication schematic of flexible supercapacitor with FCM textile electrodes and PVA/KOH gel electrolyte (**a**); digital images, capacitance retention and CV curves of supercapacitors at flat, bent and rolled-up statuses (**b**); capacitance retention and CV curves of the flexible supercapacitors after bending for 0, 50 and 100 cycles.

energy density of ACFF dropped sharply from ~85 to less than 5 μWh cm^{-2} when power density increases from ~450 to ~1600 μW cm^{-2}, while FCM ranges from 141 to 103 μWh cm^{-2} with power density from 494 to 4466 μW cm^{-2}.

Cycling stability of FCM supercapacitor at a current density of 30 mA cm^{-2} is shown in Fig. 4h. For the first 500 cycles, a slight capacitance loss of ~1% is observed. After that, an increment in capacitance occurs from ~1000 to ~3000 cycles. After 4000 cycles, the capacitance retention stabilized at ~110%. As is shown in the inset graph, curves of the 5000th and the 10000th cycle are nearly coincident. This result indicates good cycling stability of composite textiles.

A comparison was made among previous reports on flexible supercapacitors and this work and the results are shown in Table 2. Because the surface area for human body is limited, it is necessary to discuss the electrochemical performances of supercapacitors for per unit area [3]. For this work, although E_S and P_S results are not the best, the areal capacitance result and cyclic performance are inspiring. Considering the composite textiles are fabricated by such simple processes and industrial raw materials, these results are more promising and competitive. Besides, the ability to withstand deformations such as many rounds of bending is an important characteristic for flexible electrodes. The FCM electrodes were repeatedly bent from 0° to 180° as shown in Fig. 4i. 96% capacitance retained after bending for 50 cycles, and bending 100 cycles brings only about 8% capacitance degradations. After these deformations, FCM electrode keeps its original appearances, and CV curves remain an ideal rectangular shape. These results indicate the excellent flexibility of prepared textiles and suggest that the fillers adhere strongly to ACFF textiles, which are essential for roll-to-roll fabrications: a method often used for mass production of flexible energy storage devices [42–44]. Devices based on activated carbon textiles (ACT) have already been realized [45]. So, it can be inferred that with a similar 3D flexible structure and good durability when suffering deformation, the prepared composite textile electrodes are practical to be fabricated into energy storage devices by roll-to-roll manufacturing.

Solid-state flexible supercapacitors were fabricated with FCM textiles and gel electrolyte. Schematic of fabrication processes is shown in Fig. 5a, and detailed procedures are found in supporting information [41]. Digital images and CV curves of supercapacitors at different bending angles are displayed in Fig. 5b. CV curves for prepared flexible supercapacitors show great deviation from symmetric coin-cell

supercapacitors mentioned above. Because the textile electrodes are thick (~2 mm), it is difficult for electrodes to contact well with gel electrolytes. Also, pressure was added when preparing coin-cell supercapacitors, and this may cause a significant difference to the performances of textile electrodes. These problems may be easily solved by industrial fabrication methods, for example, roll-to-roll manufacturing mentioned above. CV curves of supercapacitors at different statuses are similar with each other. The capacitance retentions of supercapacitors at the bending angle of 90° and 180° are 99 and 93% compared with flat status, respectively. The flexible supercapacitor also shows good capability of bending deformation. After bending for 50 or 100 cycles, the capacitance almost keeps constant, confirming the flexibility of prepared supercapacitors. Using simple fabrication methods and structure design, MnO_2/CNT/ACFF composite textiles were prepared and ready to use as flexible supercapacitor electrodes. Considering the needs of portable and wearable devices, flexible batteries are also of great significance [46–48]. Researches have been carried out on composite textile electrodes for flexible batteries, and promising results have been achieved [49, 50]. Using the thought of structure design explained above, different fillers can be combined with the electrochemical active flexible substrates. It is possible to extend the usage of this kind of composite textiles to flexible batteries.

Conclusions

Various fabrication procedures are designed to introducing CNT and MnO_2 fillers into ACFF textiles. And the comparison of characteristics among prepared textiles was made. Electronic conductivity is found to increase with the introduction of CNTs, and introducing MnO_2/CNT fillers rather than growing MnO_2 directly on the surface of carbon fibers can improve electrochemical capacitances of composite textiles. Inspiring electrochemical performances, including areal capacitance, rate performance and cycle stability, are achieved for MnO_2/CNT/ACFF composite textiles composed by ACFF, CNTs and MnO_2/CNT fillers. Flexible supercapacitors prepared using composite textiles electrodes can be bent at different angles and endure repeated bending with little capacitance loss. As a whole, the comparison of textiles fabricated by different method may provide an idea of how to design a composite material. And composite textiles with excellent electrochemical performances and flexibility are promising for applications of high-performance flexible supercapacitor electrodes.

Acknowledgements

We acknowledge the financial support from National Key Basic Research (973) Program of China (No. 2014CB932400) and Shenzhen Technical Plan Projects (No. JCYJ20160301154114273). We also thank the financial support from CERC-CVC.

Electronic supplementary material: The online version of this article (doi:10.1007/s10853-017-0813-3) contains supplementary material, which is available to authorized users.

References

[1] Yu Z, Tetard L, Zhai L, Thomas J (2015) Supercapacitor electrode materials: nanostructures from 0 to 3 dimensions. Energy Environ Sci 8:702–730

[2] Conway BE, Pell WG (2003) Double-layer and pseudocapacitance types of electrochemical capacitors and their applications to the development of hybrid devices. J Solid State Electrochem 7:637–644

[3] Dong L, Xu C, Li Y et al (2016) Flexible electrodes and supercapacitors for wearable energy storage: a review by category. J Mater Chem A 4:4659–4685

[4] Lee JA, Shin MK, Kim SH et al (2013) Ultrafast charge and discharge biscrolled yarn supercapacitors for textiles and microdevices. Nat Commun 4:1970

[5] Fu Y, Cai X, Wu H et al (2012) Fiber supercapacitors utilizing pen ink for flexible/wearable energy storage. Adv Mater 24:5713–5718

[6] Yu D, Qian Q, Wei L et al (2015) Emergence of fiber supercapacitors. Chem Soc Rev 44:647–662

[7] Nyholm L, Nyström G, Mihranyan A et al (2011) Toward flexible polymer and paper-based energy storage devices. Adv Mater 23:3751–3769

[8] Meng C, Liu C, Fan S (2009) Flexible carbon nanotube/polyaniline paper-like films and their enhanced electrochemical properties. Electrochem Commun 11:186–189

[9] Yan X, Tai Z, Chen J et al (2011) Fabrication of carbon nanofiber-polyaniline composite flexible paper for supercapacitor. Nanoscale 3:212–216

[10] Jost K, Perez CR, McDonough JK et al (2011) Carbon coated textiles for flexible energy storage. Energy Environ Sci 4:5060–5067

[11] Jost K, Dion G, Gogotsi Y (2014) Textile energy storage in perspective. J Mater Chem A 2:10776–10787

[12] Bao L, Li X (2012) Towards textile energy storage from cotton T-shirts. Adv Mater 24:3246–3252

[13] Gao Z, Yang W, Wang J et al (2015) Flexible all-solid-state hierarchical $NiCo_2O_4$/porous graphene paper asymmetric supercapacitors with an exceptional combination of electrochemical properties. Nano Energy 13:306–317

[14] Ji J, Zhang LL, Ji H et al (2013) Nanoporous Ni $(OH)_2$ thin film on 3D ultrathin-graphite foam for asymmetric supercapacitor. ACS Nano 7:6237–6243

[15] Lei D, Song KH, Li XD et al (2017) Nanostructured polyaniline/kenaf-derived 3D porous carbon materials with high cycle stability for supercapacitor electrodes. J Mater Sci. doi:10.1007/s10853-016-0504-5

[16] Gao Z, Song N, Zhang Y et al (2015) Cotton textile enabled, all-solid-state flexible supercapacitors. RSC Adv 5:15438–15447

[17] Zhou W, Cao X, Zeng Z et al (2013) One-step synthesis of Ni_3S_2 nanorod@ $Ni(OH)_2$ nanosheet core-shell nanostructures on a three-dimensional graphene network for high-performance supercapacitors. Energy Environ Sci 6:2216–2221

[18] Gao Z, Song N, Li X (2015) Microstructure design of hybrid CoO@ NiO and graphene nano-architectures for flexible high performance supercapacitors. J Mater Chem A 3:14833–14844

[19] Hsu YK, Chen YC, Lin YG et al (2012) High-cell-voltage supercapacitor of carbon nanotube/carbon cloth operating in neutral aqueous solution. J Mater Chem 22:3383–3387

[20] Zhao Y, Liu J, Hu Y et al (2013) Highly compression-tolerant supercapacitor based on polypyrrole-mediated graphene foam electrodes. Adv Mater 25:591–595

[21] Dubal DP, Kim JG, Kim Y et al (2014) Supercapacitors based on flexible substrates: an overview. Energy Technol 2:325–341

[22] Yuan L, Lu XH, Xiao X et al (2011) Flexible solid-state supercapacitors based on carbon nanoparticles/MnO_2 nanorods hybrid structure. ACS Nano 6:656–661

[23] Hu L, Pasta M, Mantia FL et al (2010) Stretchable, porous, and conductive energy textiles. Nano Lett 10:708–714

[24] He Y, Chen W, Li X et al (2012) Freestanding three-dimensional graphene/MnO_2 composite networks as ultralight and flexible supercapacitor electrodes. ACS Nano 7:174–182

[25] Dong L, Xu C, Li Y et al (2016) Simultaneous production of high-performance flexible textile electrodes and fiber electrodes for wearable energy storage. Adv Mater 28:1675–1681

[26] Dong L, Xu C, Yang Q et al (2015) High-performance compressible supercapacitors based on functionally synergic multiscale carbon composite textiles. J Mater Chem A 3:4729–4737

[27] Chmiola J, Largeot C, Taberna PL et al (2010) Monolithic carbide-derived carbon films for micro-supercapacitors. Science 328:480–483

[28] Liu W, Yan X, Lang J et al (2012) Flexible and conductive nanocomposite electrode based on graphene sheets and cotton cloth for supercapacitor. J Mater Chem 22:17245–17253

[29] Bélanger D, Brousse L, Long JW (2008) Manganese oxides: battery materials make the leap to electrochemical capacitors. Electrochem Soc Interface 17:49–52

[30] Bello A, Fashedemi OO, Lekitima JN et al (2013) High-performance symmetric electrochemical capacitor based on graphene foam and nanostructured manganese oxide. AIP Adv 3:082118

[31] Tao J, Liu N, Li L et al (2014) Hierarchical nanostructures of polypyrrole@ MnO_2 composite electrodes for high performance solid-state asymmetric supercapacitors. Nanoscale 6:2922–2928

[32] Ma SB, Nam KW, Yoon WS et al (2008) Electrochemical properties of manganese oxide coated onto carbon nanotubes for energy-storage applications. J Power Sources 178:483–489

[33] Ma SB, Ahn KY, Lee ES et al (2007) Synthesis and characterization of manganese dioxide spontaneously coated on carbon nanotubes. Carbon 45:375–382

[34] Li P, Yang Y, Shi E et al (2014) Core-double-shell, carbon nanotube@ polypyrrole@ MnO_2 sponge as freestanding, compressible supercapacitor electrode. ACS Appl Mater Interfaces 6:5228–5234

[35] Jin X, Zhou W, Zhang S et al (2007) Nanoscale microelectrochemical cells on carbon nanotubes. Small 3:1513–1517

[36] Dong L, Hou F, Zhong X et al (2013) Comparison of drying methods for the preparation of carbon fiber felt/carbon nanotubes modified epoxy composites. Compos A 55:74–82

[37] Frackowiak E, Metenier K, Bertagna V et al (2000) Supercapacitor electrodes from multiwalled carbon nanotubes. Appl Phys Lett 77:2421–2423

[38] Zhao X, Chu BTT, Ballesteros B et al (2009) Spray deposition of steam treated and functionalized single-walled and multi-walled carbon nanotube films for supercapacitors. Nanotechnol 20:065605

[39] Zhang L, Aboagye A, Kelkar A et al (2014) A review: carbon nanofibers from electrospun polyacrylonitrile and

their applications. J Mater Sci 49:463–480. doi:10.1007/s10853-013-7705-y

[40] Taberna PL, Simon P, Fauvarque JF (2003) Electrochemical characteristics and impedance spectroscopy studies of carbon-carbon supercapacitors. J Electrochem Soc 150:A292–A300

[41] Dong L, Xu C, Li Y et al (2016) Breathable and wearable energy storage based on highly flexible paper electrodes. Adv Mater 28:9313–9319

[42] Huang Y, Chen J, Yin Z et al (2011) Roll-to-roll processing of flexible heterogeneous electronics with low interfacial residual stress. IEEE Trans Compon Packag Manuf Technol 1:1368–1377

[43] Pasta M, La Mantia F, Hu L et al (2010) Aqueous supercapacitors on conductive cotton. Nano Res 3:452–458

[44] Yuan C, Hou L, Li D et al (2011) Synthesis of flexible and porous cobalt hydroxide/conductive cotton textile sheet and its application in electrochemical capacitors. Electrochim Acta 56:6683–6687

[45] Gao Z, Bumgardner C, Song N et al (2016) Cotton-textile-enabled flexible self-sustaining power packs via roll-to-roll fabrication. Nat Commun 7:11586

[46] Liu W, Song MS, Kong B et al (2016) Flexible and stretchable energy storage: recent advances and future perspectives. Adv Mater. doi:10.1002/adma.201603436

[47] Shen L, Ding B, Nie P et al (2013) Advanced energy-storage architectures composed of spinel lithium metal oxide nanocrystal on carbon textiles. Adv Energy Mater 3:1484–1489

[48] Gao Z, Song N, Zhang Y et al (2015) Cotton-textile-enabled, flexible lithium-ion batteries with enhanced capacity and extended lifespan. Nano Lett 15:8194–8203

[49] Liu B, Zhang J, Wang X et al (2012) Hierarchical three-dimensional $ZnCo_2O_4$ nanowire arrays/carbon cloth anodes for a novel class of high-performance flexible lithium-ion batteries. Nano Lett 12:3005–3011

[50] Gao Z, Zhang Y, Song N et al (2016) Biomass-derived renewable carbon materials for electrochemical energy storage. Mater Res Lett. doi:10.1080/21663831.2016.1250834